Inorganic Chemistry

Forum Article

pubs.acs.org/IC

Free Reaction Enthalpy Profile of the Schrock Cycle Derived from Density Functional Theory Calculations on the Full [Mo^{HIPT}N$_3$N] Catalyst

Wulf Thimm,[†] Christian Gradert,[†] Henning Broda,[†] Frank Wennmohs,[‡] Frank Neese,*[,‡] and Felix Tuczek*[,†]

[†]Institut für Anorganische Chemie, Christian-Albrechts-Universität zu Kiel, Max-Eyth-Straße 2, D-24118 Kiel, Germany

[‡]Max-Planck-Institut für chemische Energiekonversion, Stiftstraße 34-36, D-45470 Mülheim an der Ruhr, Germany

Supporting Information

ABSTRACT: A series of density functional theory (DFT) calculations on the full [Mo^{HIPT}N$_3$N] catalyst are performed to obtain an energy profile of the Schrock cycle. This is a continuation of our earlier investigation of this cycle in which the bulky hexaisopropyterphenyl (HIPT) substituents of the ligand were replaced by hydrogen atoms (*Angew. Chem., Int. Ed.* **2005**, *44*, 5639). In an effort to provide a treatment that is as converged as possible from a quantum-chemical point of view, the present study now fully takes the HIPT moieties into account. Moreover, structures and energies are calculated with a near-saturated basis set, leading to models with 280 atoms and 4850 basis functions. Solvent and scalar relativistic effects have been treated using the conductor-like screening model and zeroth-order regular approximation, respectively. Free reaction enthalpies are evaluated using the PBE and B3LYP functionals. A comparison to the available experimental data reveals much better agreement with the experiment than preceding DFT treatments of the Schrock cycle. In particular, free reaction enthalpies of reduction steps and NH_3/N_2 exchange are now excellently reproduced.

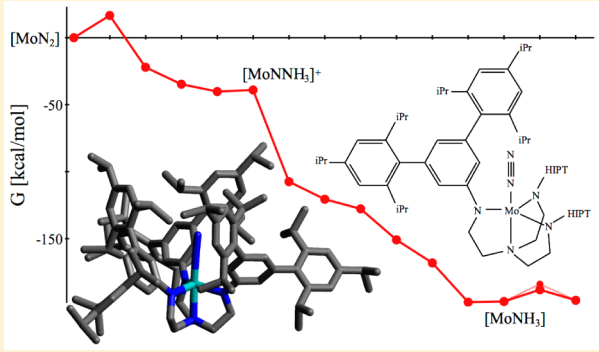

INTRODUCTION

Almost every nitrogen atom in living organisms has gone through either biological nitrogen fixation or the Haber−Bosch process. Both reactions, one natural and the other one man-made, produce comparable amounts of ammonia from atmospheric dinitrogen (N_2) worldwide (about 100 million tons/year).[1] Whereas details of the Haber−Bosch process have been elucidated on an atomic level,[2] the molecular mechanism of the biological reaction is still not fully understood.[3−5] A third scenario, synthetic nitrogen fixation, involves the activation of N_2 and its stepwise conversion to ammonia by transition-metal complexes in homogeneous solution.[6] Only three systems exist that achieve this reaction in a catalytic fashion.[7−9] One of them is based on the molybdenum(III) complex [Mo(N_2)-(^{HIPT}N$_3$N)] supported by a triamidoamine ligand (HIPT = hexaisopropylterphenyl, 3,5-(2,4,6-^{i}Pr$_3$C$_6$H$_2$)$_2$C$_6$H$_3$).[7,10−19] Using this complex as a catalyst, LutHBAr$^{F}_4$ [Lut = 2,6-dimethylpyridine; Ar^{F} = 3,5-(CF$_3$)$_2$C$_6$H$_3$] as a proton source, and decamethylchromocene as a reductant, Yandulov and Schrock were able to generate 8 equiv (four turnovers) of ammonia with an efficiency of 66% with respect to the reducing equivalents. The isolation and characterization of key intermediates of this cycle allowed the formulation of a concise reaction mechanism (Figure 1).

Several years ago, we have derived a detailed free reaction enthalpy profile of the Schrock cycle from density functional theory (DFT) calculations.[20,21] In this original contribution, the nitrogen-containing intermediates were modeled by replacing the HIPT substituents of the ^{HIPT}N$_3$N ligand with hydrogen atoms (cf. Figure 2a). The involved reagents and reaction products were treated at the same level as the Mo−N$_x$H$_y$ species (x = 1, 2; y = 0−3). Geometry optimizations were performed using the, at the time, most commonly employed approach, namely, DFT with the B3LYP[22] functional and the effective-core-potential-based LANL2DZ basis set. Electronic energies were determined using B3LYP/TZVP. A solvent correction was included for heptane, based on the polarizable continuum model (PCM). Importantly, these calculations suggested a strictly alternating sequence of protonation and reduction steps, in agreement with the experimental observation.[16] Moreover, it could be inferred from the calculations that the most endergonic step is the first protonation of the coordinated N_2 ligand and the most exergonic step the cleavage

Special Issue: Small Molecule Activation: From Biological Principles to Energy Applications

Received: April 14, 2015
Published: June 24, 2015

DOI: 10.1021/acs.inorgchem.5b00787
Inorg. Chem. 2015, 54, 9248−9255

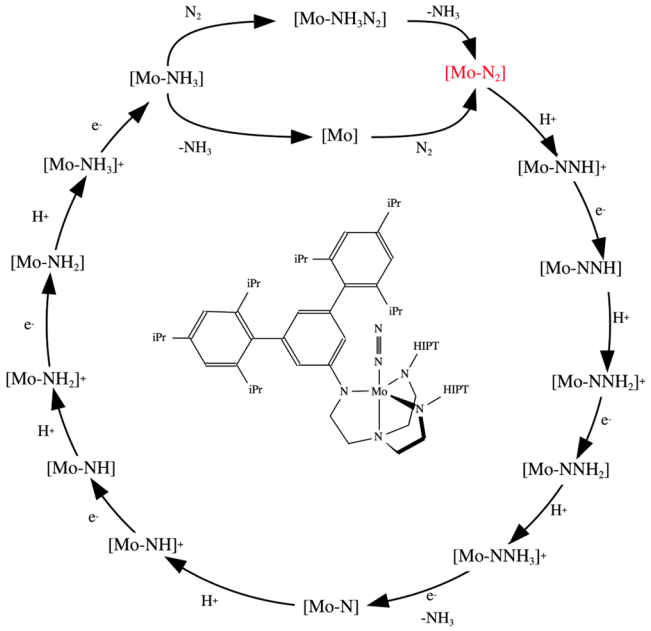

Figure 1. Mechanism of the Schrock cycle.

of the N−N bond at the molybdenum hydrazidium stage. The overall exergonicity of the process was found to be very large but on the same order of magnitude as the biological process (about 180 kcal/mol of N_2).[20]

A number of other theoretical treatments of the energetics of the Schrock cycle and related systems have appeared that, in part, considered larger models of the catalysts.[23−36] On the basis of a model of the [Mo($^{HIPT}N_3N$)] complex, where the HIPT residues are replaced by phenyl groups (Figure 2b), Cao et al. treated all intermediates of the Schrock cycle (N_2, NNH^+, ..., NH_3) with DFT, employing the BLYP functional.[23] Moreover, ammonium (NH_4^+) was considered as the proton source and an iron−sulfur cluster as the electron donor. The resulting energy profile is much more exothermic (−370 kcal/mol for one reactive cycle) than ours. On the other hand, it exhibits highly endothermic steps of up to 73 kcal/mol, in contrast to the thermally allowed reaction course observed experimentally. Magistrato and Robertazzi (M&R) also used a model of the Schrock catalyst based on a phenyl-terminated $^{HIPT}N_3N$ ligand.[24,25] Analogous to our treatment, lutidinium and decamethylchromocene were explicitly considered as the proton source and reductant, respectively. Reaction energies were calculated for all protonation and reduction steps based on a triple-ζ Slater-type orbital (STO) basis set for molybdenum and a double-ζ STO basis set for all other atoms, employing the BP86 functional along with a solvent correction based on the PCM. In agreement with the experiment, an energy profile consisting of thermally allowed elementary reactions was derived. However, large discrepancies (17−18 kcal/mol) between experimentally determined reaction enthalpies and calculated reaction energies were noticed, in particular for the protonation steps. Therefore, the effect of a number of explicit solvent molecules was explored, for both the proton source and the catalyst model. Whereas inclusion of at most two solvent molecules for the molybdenum species was computationally feasible, up to four solvent molecules were included for the proton source. By this approach, the discrepancy between experimental free energies and calculated reaction energies could be reduced to less than ∼5 kcal/mol for the protonation steps. On the other hand, no significant influence of an explicit solvation model on the energetics of the reduction steps was detected.

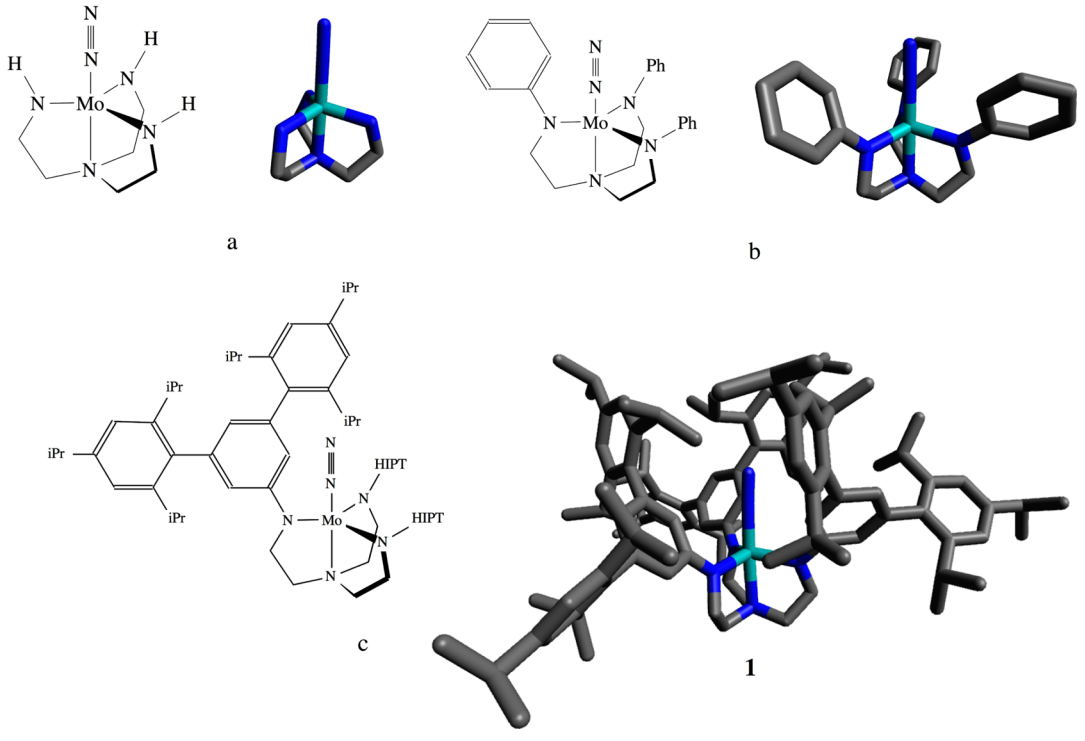

Figure 2. Models of the [Mo(N_2)($^{HIPT}N_3N$)] complex: (a) hydrogen-terminated ligand; (b) phenyl-terminated ligand; (c) full HIPT-substituted ligand. **1**: optimized structure of the N_2 complex.

DOI: 10.1021/acs.inorgchem.5b00787
Inorg. Chem. 2015, 54, 9248−9255

Table 1. Gibbs Free Enthalpies ΔG of $[Mo(^{HIPT}N_3N)]$ Calculated with the PBE and B3LYP Functionals and the def2-TZVP Basis Set Including Solvent Correction[a]

	ΔE			ΔG			ΔE		
reaction	B3LYP/ def2-TZVP	PBE/ def2-TZVP	thermal correction to ΔG	B3LYP/ def2-TZVP	PBE/ def2-TZVP	Studt et al.[20]	M&R[24]	Reiher et al.[28]	ΔG expt.
$N_2 + 3H_2 \rightarrow 2NH_3$	−40.6	−45.0	30.7	**−9.9**	−14.3				
$Cp^*_2Cr \rightarrow Cp^*_2Cr^+ / C \rightarrow C^+$	87.9	95.2	−0.4	**87.5**	94.8				
$LutH^+ \rightarrow Lut / LH^+ \rightarrow L$	258.6	257.1	−8.4	**250.2**	248.7				
$[Mo] + N_2 \rightarrow [Mo\text{-}N_2]$	−24.4	−35.2	12.3	**−12.1**	−22.9	−14.2	−29	−36.1	
$[Mo\text{-}N_2] + LH^+ \rightarrow [Mo\text{-}NNH]^+ + L$	16.6	7.2	0.0	**16.6**	7.2	21.1	+4	−0.7	
$[Mo\text{-}NNH]^+ + C \rightarrow [Mo\text{-}NNH] + C^+$	−38.4	−28.7	−0.3	**−38.7**	−29.0	−39.4	−35	−14.6	
$[Mo\text{-}NNH] + LH^+ \rightarrow [Mo\text{-}NNH_2]^+ + L$	−12.9	−12.6	0.3	**−12.6**	−12.3	−10.2	−17	−22.0	−0.28
$[Mo\text{-}NNH_2]^+ + C \rightarrow [Mo\text{-}NNH_2] + C^+$	−2.5	8.2	−3.0	**−5.5**	5.2	0.7	+7	+22.2	−4 to −7
$[Mo\text{-}NNH_2] + LH^+ \rightarrow [Mo\text{-}NNH_3]^+ + L$	0.3	0.9	0.9	**1.2**	1.8	−1.5	−2	−9.3	
$[Mo\text{-}NNH_3]^+ + C \rightarrow [Mo\text{-}N] + NH_3 + C^+$	−53.3	−43.9	−15.1	**−68.4**	−59.0	−72.8	−51	−39.2	
$[Mo\text{-}N] + LH^+ \rightarrow [Mo\text{-}NH]^+ + L$	−11.1	−12.6	−2.0	**−13.1**	−14.6	−13.2	−17	−20.3	+1.35
$[Mo\text{-}NH]^+ + C \rightarrow [Mo\text{-}NH] + C^+$	−5.6	4.7	−1.6	**−7.2**	3.1	−11.3	+5	+18.4	−5 to −6
$[Mo\text{-}NH] + LH^+ \rightarrow [Mo\text{-}NH_2]^+ + L$	−22.1	−21.0	−1.0	**−23.1**	−22.0	−26.2	−29	−35.1	
$[Mo\text{-}NH_2]^+ + C \rightarrow [Mo\text{-}NH_2] + C^+$	−15.1	−2.5	−2.1	**−17.2**	−4.6	−17.1	−2	+10.0	
$[Mo\text{-}NH_2] + LH^+ \rightarrow [Mo\text{-}NH_3]^+ + L$	−30.7	−28.1	1.4	**−29.3**	−26.7	−25.7	−35	−21.2	
$[Mo\text{-}NH_3]^+ + C \rightarrow [Mo\text{-}NH_3] + C^+$	2.3	9.3	−1.8	**0.5**	7.5	+2.6	+8	+4.5	0 to +1
$[Mo\text{-}NH_3] + N_2 \rightarrow [Mo\text{-}NH_3N_2]$	−5.0	−15.3	13.8	**8.8**	−1.5			−6.5	
$[Mo\text{-}NH_3N_2] \rightarrow [Mo\text{-}N_2] + NH_3$	7.1	7.7	−15.0	**−7.9**	−7.3				
$[Mo\text{-}NH_3] \rightarrow [Mo] + NH_3$	26.5	27.6	−13.5	**13.0**	14.1	+8.8	+21		
$[Mo\text{-}NH_3] + N_2 \rightarrow [Mo\text{-}N_2] + NH_3$	2.1	−7.6	−1.2	**0.9**	−8.8	−5.4	−8	−9.8	+1.4

[a]Also given are the results of Studt et al.,[20] M&R, and Reiher et al. and experimental values. All values are in kcal/mol (in this table, Cp^*_2Cr is abbreviated as C and Lut as L).

Reiher and co-workers published a series of papers in which they considered larger models of the molybdenum triamidoamine complex, employing lutidinium as acid and metallocenes (Cp^*_2Cr, Cp_2Co, etc.) as reductants.[26−31] Employing the TZVP basis set along with the BP86 functional and taking into account a model of the catalyst with the full $^{HIPT}N_3N$ ligand (Figure 2c), a complete energy profile of the Schrock cycle was derived.[28,29] Protonation and reduction energies were calculated on the basis of intrinsic proton affinities and ionization energies, respectively. Importantly, these studies provided more detailed insight into the intimate mechanisms of key steps of the Schrock cycle, in particular protonation of the N_2 complex and NH_3/N_2 exchange. Discrepancies between the calculated and experimentally determined reaction enthalpies were, however, found to be larger than those in the previous treatments, which had employed smaller models.[16,37,38]

In order to address this problem, we decided to reinvestigate the energetics of the Schrock cycle. In this study, it is attempted to provide results that are as converged as possible from the quantum-chemical point of view, given the size and complexity of the real system (see Computational Details). The proton- and electron-transfer steps are treated in the same fashion as they were previously by Studt et al. for the hydrogen-terminated ligand and M&R for the phenyl-terminated ligand.[20,39] The resulting energy profile is analyzed with respect to earlier treatments of the energetics of the Schrock cycle and the available experimental data.

COMPUTATIONAL DETAILS

For all computations, the computational chemistry program package *ORCA 3.0* was used.[40] Full models of the catalyst and $[Mo(^{HIPT}N_3N)\text{-}N_xH_y]$ complexes (x = 1, 2; y = 0−3), respectively, are used throughout (278−284 atoms). Given its excellent performance in this area,[41] geometries have been optimized with the PBE functional[42] in conjunction with a large atomic orbital basis set (def2-TZVP[43]) in the segmented all-electron relativistic (SARC) recontraction,[44] (leading to 4850 basis functions), the Split-RI-J approximation,[45] using the def2-TZVP/J[46] auxiliary basis set (7740 auxiliary basis functions), van der Waals corrections (D3BJ),[47] an explicit treatment of the scalar relativistic effects (ZORA[48]), and solvation effects using the conductor-like screening model (COSMO,[49] using heptane, ε = 1.844, as the solvent throughout). Furthermore, in order to allow a direct comparison to the available experimental data, free reaction enthalpies were calculated. This requires calculation of the harmonic vibrational frequencies, which, given the size of the system, is a time-consuming calculation that has not been attempted for the full system in previous work. Here, we provide vibrational frequencies for all species involved in the catalytic cycle. However, in order to keep turnaround times within reasonable limits, the slightly smaller def2-SVP basis set had to be used for frequency calculations based on geometry optimizations on the same level. The corresponding zero-point, thermal, and entropic corrections (all calculated at T = 298.15 K and P = 1 atm) can account for up to 15 kcal/mol in the final reaction energies. Final electronic energies are calculated with the def2-TZVP basis set in conjunction with all other corrections mentioned above but taking advantage of the higher intrinsic accuracy of the hybrid B3LYP functional relative to nonhybrid functionals such as PBE. Here, the RIJCOSX approximation[50] has been used in order to accelerate the calculation. The B3LYP functional has previously been found to reliably reproduce the electronic structures, spectroscopic properties, and reactivities of a large number of $Mo\text{−}N_xH_y$ intermediates, both of the Schrock and Chatt cycles.[51−63] Self-consistent-field (SCF) convergence was accelerated using the KDIIS and SOSCF methods.[64,65] The spin states of the complexes correspond to those of previous calculations[20,24,27] and are specified in Table S1 in the Supporting Information (SI).

DOI: 10.1021/acs.inorgchem.5b00787
Inorg. Chem. 2015, 54, 9248−9255

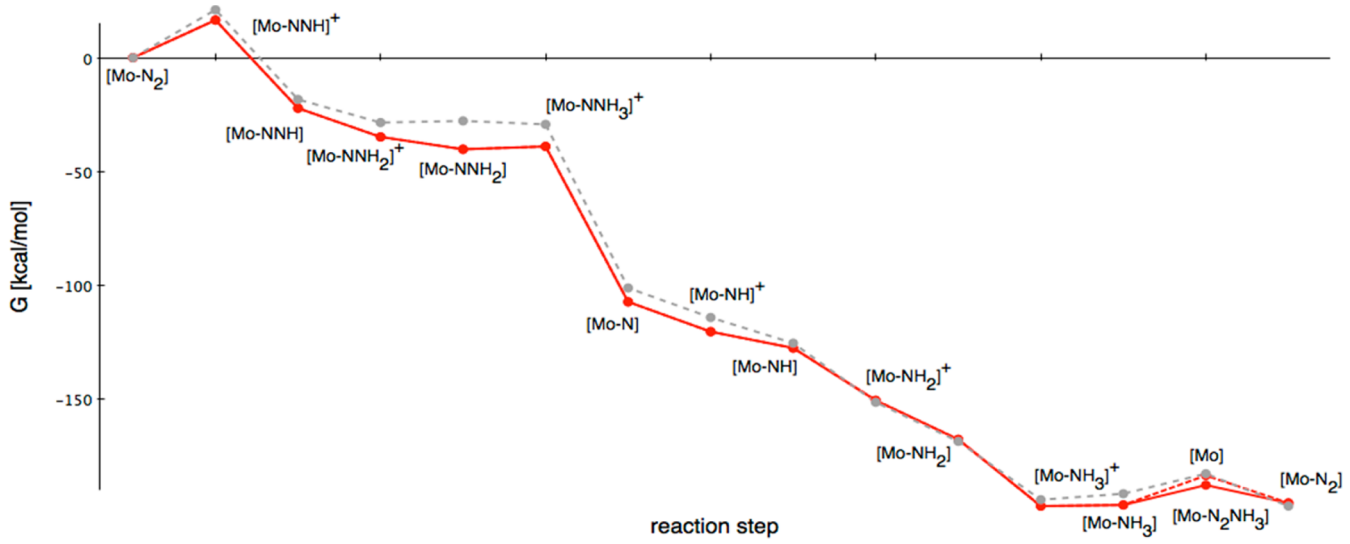

Figure 3. Gibbs free enthalpy ΔG^0 scheme of the Schrock cycle calculated with the B3LYP functional and the def2-TZVP basis set including solvent correction. Gray: calculations by Studt et al.

RESULTS AND ANALYSIS

The optimized PBE/def2-TZVP geometry of the full [Mo($^{HIPT}N_3N$)(N_2)] complex (**1**) is shown in Figure 2c. Bond distances and angles of **1** and the corresponding [Mo-N_xH_y] species treated in an analogous fashion are collected and compared to experimental values and previous calculations in Table S1 in the SI. A comparison between PBE/def2-SVP calculated and experimental frequencies is given in Table S2 in the SI. Free reaction enthalpies calculated for the formation of **1** from [Mo] + N_2 and the six protonation/reduction steps converting **1** to the intermediates of the Schrock cycle and NH_3, respectively, are collected in Table 1. These calculations are based on electronic energies obtained with B3LYP/def2-TZVP and PBE/def2-TZVP, respectively, with thermal corrections being derived from frequency calculations at the PBE/def2-SVP level. All protonations and reductions are supposed to be mediated by lutidinium and decamethylchromocene, respectively. The energy profile resulting from the B3LYP/def2-TZVP calculation is shown in Figure 3. For comparison, free reaction enthalpies resulting from calculations of Studt et al. are given in Table 1 and indicated in Figure 3 as well. As mentioned in the Introduction, this energy profile has been derived based on single-point energies employing B3LYP/TZVP, using a simplified model of the catalyst with a hydrogen-terminated N_3N ligand (Figure 2a).[20] Furthermore, reaction energies determined by M&R[24] as well as Reiher et al.[29] are collected Table 1; these have been determined on the basis of phenyl-terminated and full $^{HIPT}N_3N$ ligands, respectively (Figure 2b,c). Finally, experimentally determined free reaction enthalpies are indicated in Table 1 for selected reaction steps; all energies are given in kcal/mol.

As is evident from Table 1 and Figure 3, bonding of N_2 to the four-coordinate [Mo($^{HIPT}N_3N$)] (≡[Mo]) complex is quite exergonic (B3LYP, −12.1 kcal/mol; PBE, −22.9 kcal/mol), with the B3LYP value for **1** being fairly similar to that obtained by Studt et al. on the truncated model (−14.2 kcal/mol). Interestingly, the PBE reaction energy (−35.2 kcal/mol) is very close to the value obtained by Reiher et al. on the full model (−36.1 kcal/mol), employing BP86. Because of the loss of entropy upon N_2 binding to **1**, the thermal correction energy is quite substantial for this reaction (+12.1 kcal/mol). Unfortunately, no direct experimental information regarding the free reaction enthalpy of N_2 binding is available. Nevertheless, it is known that the conversion of [Mo-$^{15}N_2$] to [Mo-N_2] under a N_2 pressure of 15 psi proceeds with a rate of $k = 5.3 \times 10^{-6}$ s^{-1} (half-life of 36 h), presumably via a four-coordinate [Mo] intermediate.[11] This would correspond to a free activation energy $\Delta G^{\ddagger}$ of 24.8 kcal/mol for N_2 loss, which is about twice as large as the free N_2-binding/dissociation enthalpy calculated here. The difference between the free activation enthalpy and free dissociation enthalpy might be due to the fact that the free ligand has to leave the cage generated by the bulky HIPT groups, introducing an additional barrier to N_2 loss. Further information with respect to the thermodynamics of N_2 binding has been determined for the NH_3/N_2 exchange reaction, which will be considered below.

For the first protonation of bound N_2, a large positive free reaction enthalpy is calculated by B3LYP (+16.6 kcal/mol), which again is reasonably close to the calculation of Studt et al. (+21.1 kcal/mol). This result is in agreement with the high thermodynamic instability of [Mo-NNH]$^+$.[12] The PBE value (+7.2 kcal/mol) is much lower and qualitatively agrees with the reaction energy obtained by M&R (+4 kcal/mol). Reiher et al. have obtained a slightly negative reaction energy for the first protonation step (−0.7 kcal/mol). Because there is no experimental indication that the N_2 ligand of **1** is directly protonated,[12,16] this result would indicate that protonation of coordinated N_2 is *kinetically* hindered in **1** (thermal correction is very small for this step; cf. Table 1). This prompted Reiher et al. to investigate an alternative pathway in which one of the amide donors of the $^{HIPT}N_3N$ ligand is protonated first;[28] this species could, in fact, be detected experimentally.[21] Subsequently, a one-electron reduction occurs, and the proton is transferred from the amide group to the coordinated N_2 ligand, eventually catalyzed by a second proton. Our result of a strongly positive free protonation enthalpy of coordinated N_2 would account for such an indirect pathway because in this case the complex would avoid a *thermodynamically* unfavorable first protonation of the N_2 ligand. In contrast to the latter reaction step, subsequent reduction of the resulting [Mo-NNH]$^+$ complex is predicted to be strongly exergonic (B3LYP, −38.8 kcal/mol; PBE, −29.1 kcal/mol). In qualitative agreement with

DOI: 10.1021/acs.inorgchem.5b00787
Inorg. Chem. 2015, 54, 9248−9255

our results, M&R obtained a reaction energy of −35 kcal/mol, whereas Reiher et al. reported a significantly smaller value (−14.6 kcal/mol).

For the second protonation of the N_2 complex, both B3LYP and PBE indicate a free reaction enthalpy of about −12.5 kcal/mol, which agrees well with the value obtained by Studt et al. (−10.2 kcal/mol). From the experimentally determined equilibrium constant of K_{eq} = 1.6, this reaction is found to be thermoneutral (ΔG° = −0.28 kcal/mol).[12] Therefore, an error of 12−13 kcal/mol between the theory and experiment has to be noted. Even larger discrepancies were obtained by M&R and Reiher et al., who determined reaction energies of −17 and −22.0 kcal/mol, respectively. M&R thus explored the explicit incoporation of solvent molecules for the acid and molybdenum complexes (vide supra), eventually reducing the discrepancy between the theory and experiment to ∼5 kcal/mol.

The subsequent reduction of the $[Mo\text{-}NNH_2]^+$ complex to $[Mo\text{-}NNH_2]$ is experimentally found to proceed spontaneously with three metallocenes (Cp_2Co, Cp^*_2Cr, and Cp^*_2Co) in C_6D_6. Considering the fact that the redox potential of Cp_2Co is less negative by 0.14−0.3 V than that of Cp^*_2Cr (depending on the solvent),[12] one can conclude that for Cp^*_2Cr this reaction should be exergonic by at least −4 to −7 kcal/mol. This confirms our B3LYP result (−5.4 kcal/mol), whereas PBE predicts the reaction to be endergonic (+5.2 kcal/mol). Studt et al. obtained a free reaction enthalpy of +0.7 kcal/mol for this reaction, whereas M&R find a moderately endothermic behavior (+7 kcal/mol), close to our PBE result. By contrast, Reiher et al. calculated this reaction to be strongly endothermic (+22 kcal/mol).

The energy for the third protonation of complex-bound N_2 is found to be slightly endergonic (1−2 kcal/mol) for both B3LYP and PBE. Studt et al. and M&R obtained slightly negative energies (−1.5 and −2 kcal/mol, respectively), whereas Reiher et al. determined an even larger negative value (−9.3 kcal/mol). Upon subsequent transfer of an electron to the $[Mo\text{-}NNH_3]^+$ complex, the N−N bond is cleaved and the first molecule of ammonia is released under formation of the nitrido complex. For both B3LYP and PBE, this reaction is found to be strongly exergonic (−68.4 and −59.0 kcal/mol, respectively). This qualitatively agrees with the theoretical result of Studt (−72.8 kcal/mol) and large exothermicities evidenced for the N−N cleavage of Mo hydrazidium complexes with phosphine coligands.[56] Somewhat less exothermic reactions were calculated by M&R (−51 kcal/mol) and Reiher et al. (−39.2 kcal/mol), whereby it has to be taken into account that the thermal correction for this reaction step amounts to −15 kcal/mol. This leads to similar free reaction enthalpies for N−N splitting as obtained in our calculations.

The second part of the Schrock cycle starts with protonation of the nitrido complex. For this reaction, free reaction enthalpies of −13.1 kcal/mol (B3LYP) and −14.6 kcal/mol (PBE) are obtained. Studt et al. found an energy of −13.2 kcal/mol, essentially identical with the B3LYP result, whereas M&R and Reiher et al. obtained values of −17 and −20.3 kcal/mol, respectively. From the experimentally determined equilibrium constant of this reaction (K_{eq} ∼ 0.1), a ΔG° value of +1.35 kcal/mol is derived.[12] The discrepancy between the experiment and theory thus is large (≥14 kcal/mol). M&R therefore treated this reaction step with more elaborate solvent models for the acid as well, reaching better agreement with the experimental value.[24]

Subsequent reduction of the $[Mo\text{-}NH]^+$ complex by Cp^*_2Cr is experimentally found to proceed spontaneously.[12] Because the redox potential of $[Mo\text{-}NH]^+$ is less negative by 0.22−0.25 V than that of Cp^*_2Cr, free reaction enthalpies should be in the range of −5 to −6 kcal/mol with this reductant, which is matched by the B3LYP result (−7.2 kcal/mol) very well, whereas PBE gives a too endergonic reaction (+3.1 kcal/mol). Studt et al. also found a negative free reaction enthalpy (−11.3 kcal/mol), whereas M&R obtained a positive (+5 kcal/mol) reaction energy, in agreement with our PBE result. Reiher et al. calculated an even more positive value for the reaction energy (+18.4 kcal/mol).

With respect to protonation of the imido complex, fairly negative reaction enthalpies are obtained for both B3LYP (−23.0 kcal/mol) and PBE (−21.9 kcal/mol). Even more negative values have been reported by Studt et al. (free reaction enthalpy of −25.7 kcal/mol), M&R (reaction energy of −29 kcal/mol), and Reiher et al. (−35.1 kcal/mol). The subsequent reduction is calculated to be exergonic as well (B3LYP, −17.2 kcal/mol; PBE, −4.6 kcal/mol). On the basis of a thermal correction of −2.1 kcal/mol for this step, the PBE value is in good agreement with the reaction energy of −2 kcal/mol obtained by M&R, whereas Reiher et al. predicted a significantly more positive reaction energy (+10.0 kcal/mol).

Protonation of the amido complex leads to the $[Mo\text{-}NH_3]^+$ intermediate. With both B3LYP and PBE, strongly negative free reaction enthalpies are obtained for this step (−29.4 and −26.7 kcal/mol, respectively). Studt et al. found a free reaction enthalpy of −25.7 kcal/mol, whereas M&R and Reiher et al. obtained reaction energies of −35 and −21.2 kcal/mol, respectively. Reduction of the $[Mo\text{-}NH_3]^+$ complex, on the other hand, is calculated to be about thermoneutral with B3LYP (+0.5 kcal/mol). Experimentally, the $[Mo\text{-}NH_3]^+$ complex exhibits a redox potential that is equal to or −0.04 V more negative than that of Cp^*_2Cr, depending upon the solvent.[12] This would correspond to free reaction enthalpies between 0 and +1 kcal/mol, in excellent agreement with our calculations. Studt et al. obtained a free reaction enthalpy of +2.6 kcal/mol for the truncated complex, whereas our PBE calculation gives a value of +7.5 kcal/mol, in agreement with the reaction energy determined by M&R (+8 kcal/mol). A positive reaction energy was also calculated by Reiher et al. (+4.5 kcal/mol).

The last step of the Schrock cycle involves exchange of the ammine against a dinitrogen ligand. Experimentally, an equilibrium constant K_{eq} of 0.1 and a corresponding ΔG° value of +1.4 kcal/mol has been determined for this reaction.[12,16] Using B3LYP, we obtain a theoretical free reaction enthalpy of 0.9 kcal/mol, again in excellent agreement with the experiment. Studt et al. calculated a ΔG° value of −5.4 kcal/mol, whereas M&R and Reiher et al. obtained reaction energies of −8 and −9.8 kcal/mol, in qualitative agreement with our PBE result (−8.8 kcal/mol).

The N_2/NH_3 exchange reaction was also investigated in more detail by Reiher et al. on the basis of an associative mechanism.[31] Using molecular dynamics (MD) simulations, several possible pathways for the approach of N_2 to the five-coordinate molybdenum center of the $[Mo\text{-}NH_3]$ complex were explored. The MD simulations were then complemented by quantum-chemical geometry optimizations. As a result of these studies, a six-coordinate $[Mo\text{-}NH_3N_2]$ species could be identified that contains N_2 and NH_3 in the equatorial and axial positions, respectively, and exhibits an N−N stretching

DOI: 10.1021/acs.inorgchem.5b00787
Inorg. Chem. 2015, 54, 9248−9255

frequency that is different from that of the experimentally characterized five-coordinate N_2 complex.

On the basis of B3LYP, formation of the [Mo-NH_3N_2] complex from [Mo-NH_3] + N_2 requires a free reaction enthalpy of +8.8 kcal/mol, whereas the release of ammonia from the six-coordinate complex is exergonic by −7.9 kcal/mol. This has to be compared with the release of NH_3 from the [Mo-NH_3] complex being endergonic by 13.0 kcal/mol and the subsequent bonding of N_2 to [Mo], going downhill by −12.1 kcal/mol (cf. Figure 3). These results clearly support the preference of the catalytic system for an associative instead of a dissociative NH_3/N_2 exchange mechanism.[16] Formation of the six-coordinate intermediate is even more favored based on the PBE calculations (−1.5 kcal/mol) and the calculations of Reiher et al. (−6.5 kcal/mol). On the other hand, release of NH_3 from the ammine complex is endergonic by +14.1 kcal/mol in our PBE calculations.

Because of the precise reproduction of the net free NH_3/N_2 exchange enthalpy by B3LYP, the corresponding reaction profiles for dissociative and associate NH_3/N_2 exchange pathways are considered more trustworthy than those derived from PBE. The preference of B3LYP versus PBE regarding the description of NH_3/N_2 exchange is also supported by the available kinetic data. Experimentally, [Mo-NH_3] converts to [Mo-N_2] with a half-life $t_{1/2}$ of 35 min under an N_2 pressure of 1 atm.[16] With respect to the [Mo-$^{15}N_2$] → [Mo-N_2] exchange reaction proceeding via a four-coordinate intermediate (see above), the former reaction is faster by a factor of 62, corresponding to a decrease in the activation energy by ∼2.4 kcal/mol. Employing B3LYP, we find the six-coordinate intermediate [Mo-NH_3N_2] to be 4.2 kcal/mol lower in free enthalpy than the four-coordinate [Mo] complex (cf. Figure 3), whereas PBE predicts a free enthalpy difference of 15.6 kcal/mol between these two species (cf. Table 1 and Figure S1 in the SI), 6.5 times the above value. Of course, these considerations neglect additional (i.e., steric) barriers resulting from removal of a ligand from the cage generated the bulky HIPT groups (vide supra) and the addition of a sixth ligand to the coordination sphere of a sterically shielded five-coordinate complex, respectively, the magnitudes of which are not known experimentally.

DISCUSSION

In this work, the energetics of the Schrock cycle has been reexamined using DFT calculations. While the approach is similar to that of previous treatments, we have attempted here to converge the calculations, as far as possible, with respect to the technical aspects. In fact, the calculations reported here are probably among the largest DFT optimizations and frequency calculations that have been reported in a production level study to date.

Throughout, wherever possible, detailed comparisons have been made to the results of Studt et al., Reiher et al., and M&R, all of which have previously reported calculations on the entire reaction cycle. In broad terms, the calculations are consistent with each other, but large deviations of up to 10−20 kcal/mol in individual reaction steps are apparent. These can partially be traced back to the energetic reference point chosen for the calculation and the different density functionals used. Overall, where a reasonable comparison to the experiment is possible, the calculations reported in this work show the best agreement with the experiment. However, deviations of up to and exceeding 10 kcal/mol relative to the experiment have become apparent. In addition to the well-known difficulties to calculate accurate redox potentials and pK_a values with DFT methods, a critical point is certainly calculation of the reaction entropy on the basis of ideal gas laws, as is customary in quantum-chemical treatments. However, more sophisticated approaches based on first-principle MD calculations are still prohibitive for systems of the present size and complexity. Hence, error bars on the order of ∼10 kcal/mol should probably be considered as realistic in large-scale applications of DFT to transition-metal complexes. Given these uncertainties, we emphasize the enormous value of connecting theory and experiment at the level of advanced spectroscopy in the investigation of transition-metal reaction mechanisms.

Turning to the detailed results, importantly, the type of functional employed significantly influences the obtained reaction energies or free enthalpies. In general, the B3LYP profile is more exergonic and exhibits less endergonic steps than its PBE counterpart (cf. Figure S1 in the SI). A notable exception from this general trend is protonation of the N_2 complex, which is more endergonic with B3LYP than with PBE, rendering the first protonation the most endergonic step of the entire reaction profile. This would conform to the general concept of N_2 activation being exclusively required to enable the (most difficult) first protonation of the N_2 ligand, whereas all further steps are energetically less demanding.[59] Such a "special" role of the first protonation is less evident in the PBE profile.

A strong argument in favor of the B3LYP versus PBE functional is the excellent reproduction of the free NH_3/N_2 exchange enthalpy, which has not been achieved in any of the previous treatments of the Schrock cycle. The PBE calculation, by contrast, gives a value of −8.8 kcal/mol, in close agreement with the treatments of M&R and Reiher et al., which have been performed with the BP86 functional. Also, with respect to the reduction steps, B3LYP performs much better than its PBE counterpart. The three experimentally investigated free reduction enthalpies thus are excellently reproduced, also with respect to the differences between the $[Mo\text{-}NNH_2]^+$ and $[Mo\text{-}N]^+$ complexes, on the one hand (exergonic reductions by Cp^*_2Cr), and the $[Mo\text{-}NH_3]^+$ complex, on the other hand (thermoneutral to slightly endergonic reduction). With PBE, differences between calculated and measured free enthalpies of 6−9 kcal/mol are observed for these steps. Even more problematic is the prediction of free protonation enthalpies for both B3LYP and PBE. With the former functional, calculated enthalpies are still 12−14 kcal/mol below the experimental values. Nevertheless, these values are 8−9 kcal/mol closer to the experiment than previous reaction energies obtained for the full ligand system (Table 1).

In contrast to the large influence of the functional, the size of the employed model and the basis set appear to less strongly affect the calculated reaction enthalpies. The free enthalpy profile calculated by Studt et al. for a model with a hydrogen-terminated ligand system using B3LYP/TZVP (geometries from B3LYP/LANL2DZ)[20] is in reasonable agreement (e.g., within ∼5 kcal/mol) with its counterpart obtained for the full model of the catalyst on the basis of B3LYP/def2-TZVP (cf. Figure 2 and Table 1). Although the two corresponding energy profiles steadily diverge along the reaction coordinate, a similar agreement is observed with respect to our PBE reaction energies and those calculated by M&R for a model with a phenyl-terminated N_3N ligand, employing BP86 (cf. Figure S2 in the SI, red and green). Larger positive and negative

DOI: 10.1021/acs.inorgchem.5b00787
Inorg. Chem. 2015, 54, 9248−9255

deviations are observed relative to the calculations of Reiher et al. (Figure S2 in the SI, blue), which have been performed with BP86 as well. Obviously, these discrepancies are not due to the functional employed but mostly to the method applied to determine the protonation and reduction energies, respectively.

The relative insensitivity of the energy profile upon the actual size of the employed ligand system can be traced back to an effective decoupling of the π systems of the aromatic substituents from the metal center of the $[Mo^{HIPT}N_3N]$ complex and its first coordination sphere. Specifically, the π lone pairs of the amide donors (which, in turn, are perpendicular to the π-back-bonding metal orbitals of the molybdenum center) are oriented within the $Mo-N(amide)_3$ plane. Because of a rotation of the attached phenyl groups out of planes perpendicular to the MoN_3 plane and containing the Mo−N axes (cf. Figure 2b,c), π overlap between the amide groups and the π systems of these substituents is small. Consequently, any further modification of these phenyl groups (e.g., by substitution with additional aryl groups) has little influence on the electronic structure of the $Mo-N_3N$ core. The only role of the bulky HIPT substituents is therefore a steric one; electronically, they could be replaced by terphenyl, phenyl, or, as the calculations have shown, even hydrogen.

SUMMARY AND CONCLUSION

In summary, an almost complete picture of the energetics of the Schrock cycle has been obtained, using state-of-the-art quantum-chemical methods along with a full model of the catalyst. Both the reduction steps and the NH_3/N_2 exchange reaction have been reproduced with an accuracy that presently is difficult to improve further. A comparable agreement with the experiment for the energetics of the protonation steps is, however, still lacking. In order to theoretically determine free protonation enthalpies at the same level of precision as that achieved for other reactions of the Schrock cycle, a more detailed quantum-chemical modeling of the proton-transfer steps, hence, appears necessary.[24]

ASSOCIATED CONTENT

Supporting Information

Free enthalpy profiles, energy profiles, bond lengths and angles, frequencies, total energies, and additional energy values. The Supporting Information is available free of charge on the ACS Publications website at DOI: 10.1021/acs.inorgchem.5b00787.

AUTHOR INFORMATION

Corresponding Authors

*E-mail: Frank.Neese@cec.mpg.de.
*E-mail: ftuczek@ac.uni-kiel.de.

Notes

The authors declare no competing financial interest.

REFERENCES

(1) Smil, V. *Enriching the Earth: Fritz Haber, Carl Bosch, and the Transformation of Food Production*; MIT Press: Cambridge, MA, 2001.
(2) Ertl, G. *Angew. Chem., Int. Ed. Engl.* **1990**, *29*, 1219−1227.
(3) Seefeldt, L. C.; Hoffman, B. M.; Dean, D. R. *Annu. Rev. Biochem.* **2009**, *78*, 701−722.
(4) Danyal, K.; Dean, D. R.; Hoffman, B. M.; Seefeldt, L. C. *Biochemistry* **2011**, *50*, 9255−9263.
(5) Hoffman, B. M.; Lukoyanov, D.; Dean, D. R.; Seefeldt, L. C. *Acc. Chem. Res.* **2013**, *46*, 587−595.
(6) For reviews, see: (a) Hinrichsen, S.; Broda, H.; Gradert, C.; Söncksen, L.; Tuczek, F. *Annu. Rep. Prog. Chem., Sect. A: Inorg. Chem.* **2012**, *108*, 17−47. (b) MacKay, B. A.; Fryzuk, M. D. *Chem. Rev.* **2004**, *104*, 385−401. (c) Tanabe, Y.; Nishibayashi, Y. *Coord. Chem. Rev.* **2013**, *257*, 2551−2564. (d) Jia, H.-P.; Quadrelli, E. *Chem. Soc. Rev.* **2014**, *43*, 547−564.
(7) Yandulov, D. V.; Schrock, R. R. *Science* **2003**, *301*, 76−78.
(8) Anderson, J. S.; Rittle, J.; Peters, J. C. *Nature* **2013**, *501*, 84−87.
(9) Arashiba, K.; Miyake, Y.; Nishibayashi, Y. *Nat. Chem.* **2011**, *3*, 120−125.
(10) Yandulov, D. V.; Schrock, R. R. *J. Am. Chem. Soc.* **2002**, *124*, 6252−6253.
(11) Yandulov, D. V.; Schrock, R. R.; Rheingold, A. L.; Ceccarelli, C.; Davis, W. M. *Inorg. Chem.* **2003**, *42*, 796−813.
(12) Yandulov, D. V.; Schrock, R. R. *Inorg. Chem.* **2005**, *44*, 1103−1117.
(13) Weare, W. W.; Dai, C.; Byrnes, M. J.; Chin, J.; Schrock, R. R. *Proc. Natl. Acad. Sci. U.S.A.* **2006**, *103*, 17099−17106.
(14) Schrock, R. R. *Chem. Commun.* **2003**, 2389−2391.
(15) Schrock, R. R. *Acc. Chem. Res.* **2005**, *38*, 955−962.
(16) Schrock, R. R. *Angew. Chem.* **2008**, *120*, 5594−5605.
(17) Hetterscheid, D. G. H.; Hanna, B. S.; Schrock, R. R. *Inorg. Chem.* **2009**, *48*, 8569−8577.
(18) Munisamy, T.; Schrock, R. R. *Dalton Trans.* **2012**, *41*, 130−137.
(19) Kinney, R. A.; McNaughton, R. L.; Chin, J. M.; Schrock, R. R.; Hoffman, B. M. *Inorg. Chem.* **2011**, *50*, 418−420.
(20) Studt, F.; Tuczek, F. *Angew. Chem., Int. Ed.* **2005**, *44*, 5639−5642.
(21) Neese, F. *Angew. Chem., Int. Ed.* **2006**, *45*, 196−199.
(22) Becke, A. D. *J. Chem. Phys.* **1993**, *98*, 5648−5652.
(23) Cao, Z. X.; Zhou, Z. H.; Wan, H. L.; Zhang, Q. N. *Int. J. Quantum Chem.* **2005**, *103*, 344−353.
(24) Magistrato, A.; Robertazzi, A.; Carloni, P. *J. Chem. Theory Comput.* **2007**, *3*, 1708−1720.
(25) Sgrignani, J.; Franco, D.; Magistrato, A. *Molecules* **2011**, *16*, 442−465.
(26) Le Guennic, B.; Kirchner, B.; Reiher, M. *Chem.—Eur. J.* **2005**, *11*, 7448−7460.
(27) Reiher, M.; Le Guennic, B.; Kirchner, B. *Inorg. Chem.* **2005**, *44*, 9640−9642.
(28) Schenk, S.; Le Guennic, B.; Kirchner, B.; Reiher, M. *Inorg. Chem.* **2008**, *47*, 3634−3650.
(29) Schenk, S.; Le Guennic, B.; Kirchner, B.; Reiher, M. *Inorg. Chem.* **2008**, *47*, 7934.
(30) Schenk, S.; Reiher, M. *Inorg. Chem.* **2009**, *48*, 1638−1648.
(31) Schenk, S.; Kirchner, B.; Reiher, M. *Chem.—Eur. J.* **2009**, *15*, 5073−5082.
(32) Hölscher, M.; Leitner, W. *Eur. J. Inorg. Chem.* **2006**, 4407−4417.
(33) Guha, A. K.; Phukan, A. K. *Inorg. Chim. Acta* **2010**, *363*, 3270−3273.
(34) Guha, A. K.; Phukan, A. K. *Inorg. Chem.* **2011**, *50*, 8826−8833.
(35) Balu, P.; Baskaran, S.; Kannappan, V.; Sivasankar, C. *Polyhedron* **2012**, *31*, 676−681.
(36) Baskaran, S.; Sivasankar, C. *J. Mol. Catal. A: Chem.* **2013**, *370*, 140−144.
(37) Rolff, M.; Tuczek, F. Nitrogenase and Nitrogen Activation. In *Comprehensive Inorganic Chemistry II*; Reedijk, J., Poeppelmeier, K., Eds.; Elsevier: New York, 2012.
(38) Tuczek, F. Electronic Structure Calculations: Dinitrogen Reduction in Nitrogenase and Synthetic Model Systems. In *Encyclopedia of Inorganic and Bioinorganic Chemistry*; Wiley-VCH: Berlin, 2011.
(39) Magistrato, A.; Robertazzi, A.; Carloni, P. *J. Chem. Theory Comput.* **2007**, *3* (5), 1708−1720.
(40) (a) Neese, F. *ORCA, an ab-initio density functional and semi-empirical program package*; University of Bonn: Bonn, Germany, 2007. (b) Neese, F. *WIREs Comput. Mol. Sci.* **2012**, *2*, 73−78.
(41) Jiménez Castillo, U.; Torres, A. E.; Fomine, S. *J. Mol. Model.* **2014**, *20*, 2206.

DOI: 10.1021/acs.inorgchem.5b00787
Inorg. Chem. 2015, 54, 9248−9255

(42) (a) Perdew, J. P.; Burke, K.; Ernzerhof, M. *Phys. Rev. Lett.* **1996**, *77*, 3865−3868. (b) Perdew, J. P.; Burke, K.; Ernzerhof, M. *Phys. Rev. Lett.* **1997**, *78*, 1396 (Erratum).
(43) Weigend, F.; Ahlrichs, R. *Phys. Chem. Chem. Phys.* **2005**, *7*, 3297−3305.
(44) Pantazis, D. A.; Chen, X.-Y.; Landis, C. R.; Neese, F. *J. Chem. Theory Comput.* **2008**, *4* (6), 908−919.
(45) (a) Eichkorn, K.; Treutler, H.; Öhm, H.; Häser, M.; Ahlrichs, R. *Chem. Phys. Lett.* **1995**, *240*, 283−290. (b) Eichkorn, K.; Weigend, F.; Treutler, O.; Ahlrichs, R. *Theor. Chem. Acc.* **1997**, *97*, 119−124. (c) Neese, F. *J. Comput. Chem.* **2003**, *24*, 1740−1747.
(46) Weigend, F. *Phys. Chem. Chem. Phys.* **2006**, *8*, 1057−1065.
(47) (a) Grimme, S. *J. Comput. Chem.* **2004**, *25*, 1463−1473. (b) Grimme, S. *J. Comput. Chem.* **2006**, *27*, 1787−1799. Grimme, S.; Ehrlich, S.; Goerigk, L. *J. Comput. Chem.* **2011**, *32*, 1456−1465. Grimme, S.; Antony, J.; Ehrlich, S.; Krieg, H. *J. Chem. Phys.* **2010**, *132*, 154104.
(48) (a) van Lenthe, E.; Baerends, E. J.; Snijders, J. G. *J. Chem. Phys.* **1993**, *99*, 4597−4610. (b) Pantazis, D. A.; Chen, X. Y.; Landis, C. R.; Neese, F. *J. Chem. Theory Comput.* **2008**, *4*, 908−919.
(49) Klamt, A.; Schüürmann, G. *J. Chem. Soc., Perkin Trans. 2* **1993**, 799−805.
(50) Neese, F.; Wennmohs, F.; Hansen, A.; Becker, U. *Chem. Phys.* **2009**, *356*, 98−109.
(51) Lehnert, N.; Tuczek, F. *Inorg. Chem.* **1999**, *38*, 1671−1682.
(52) Lehnert, N.; Tuczek, F. *Inorg. Chem.* **1999**, *38*, 1659−1670.
(53) Horn, K. H.; Lehnert, N.; Tuczek, F. *Inorg. Chem.* **2003**, *42*, 1076−1086.
(54) Tuczek, F. *Adv. Inorg. Chem.* **2004**, *56*, 27.
(55) Horn, K. H.; Böres, N.; Lehnert, N.; Mersmann, K.; Näther, C.; Peters, G.; Tuczek, F. *Inorg. Chem.* **2005**, *44*, 3016−3030.
(56) Mersmann, K.; Horn, K. H.; Böres, N.; Lehnert, N.; Studt, F.; Paulat, F.; Peters, G.; Ivanovic-Burmazovic, I.; van Eldik, R.; Tuczek, F. *Inorg. Chem.* **2005**, *44*, 3031−3045.
(57) Sivasankar, C.; Böres, N.; Peters, G.; Habeck, C.; Studt, F.; Tuczek, F. *Organometallics* **2005**, *24*, 5393−5406.
(58) Mersmann, K.; Hauser, A.; Lehnert, N.; Tuczek, F. *Inorg. Chem.* **2006**, *45*, 5044−5056.
(59) Studt, F.; Tuczek, F. *J. Comput. Chem.* **2006**, *27* (12), 1278−1291.
(60) Stephan, G.; Sivasankar, C.; Tuczek, F. *Chem.—Eur. J.* **2008**, *14*, 644−652.
(61) Dreher, A.; Stephan, G.; Tuczek, F. *Adv. Inorg. Chem.* **2009**, *61*, 367−405.
(62) Dreher, A.; Mersmann, K.; Näther, C.; Ivanovic-Burmazovic, I.; van Eldik, R.; Tuczek, F. *Inorg. Chem.* **2009**, *48*, 2078−2093.
(63) Dreher, A.; Meyer, S.; Sarkar, B.; Kaim, W.; Kurz, P.; Tuczek, F. *Inorg. Chem.* **2013**, *52*, 2335−2352.
(64) (a) Pulay, P. *Chem. Phys. Lett.* **1980**, *73*, 393−398. (b) Pulay, P. *J. Comput. Chem.* **1992**, *3*, 556−560.
(65) Fischer, T. H.; Almlöf, J. *J. Phys. Chem.* **1992**, *96*, 9768. (b) Neese, F. *Chem. Phys. Lett.* **2000**, *325*, 93−98.

DOI: 10.1021/acs.inorgchem.5b00787
Inorg. Chem. 2015, 54, 9248−9255